Photoinduced charge transfer in MEH-PPV/Pt$_{0.75}$C$_{60}$ donor-acceptor blends

A.A.Bakulin, S.G.Elizarov, A.E.Ozimova, D.Yu.Paraschuk,
Yu.N.Novikov[*], M.V. Tsikalova[*], S.A.Arnautov[**],
E.M.Nechvolodova[**]

M.Lomonosov Moscow State University, International Laser Center,
Leninskie Gory, 119992 Moscow, Russia
[*]A.Nesmeyanov Institute of Organoelement Compounds
Russian Academy of Sciences, 28 Vavilova Str., 119991 Moscow, Russia
[**]N.Semenov Institute of Chemical Physics Russian Academy of Sciences,
4 Kosygina Str., 119991 Moscow, Russia

Photoinduced charge transfer (PCT) in donor-acceptor blends of poly[2-methoxy-5-(2′-ethyl-hexyloxy)-1,4-phenylene vinylene] (MEH-PPV) with coordination oligomer (Pt$_{0.75}$C$_{60}$)$_n$ has been studied and compared with that in MEH-PPV/C$_{60}$ blends. The blends were investigated by using optical absorption, scattering, photoluminescence (PL), photoinduced absorption (PIA), and photocurrent action spectroscopies. We have found that he efficiency of PCT in MEH-PPV/(Pt$_{0.75}$C$_{60}$)$_n$ blend is somewhat less than in MEH-PPV/C$_{60}$. This difference is attributed to more enhanced phase separation in MEH-PPV/(Pt$_{0.75}$C$_{60}$)$_n$ at the nanoscale. Meanwhile, our photocurrent data imply that (Pt$_{0.75}$C$_{60}$)$_n$ chains could provide a network for collection of photoinduced charges.

Исследован фотоиндуцированный перенос заряда (ФПЗ) в донорно-акцепторных смесях поли[2-метокси-5-(2′-этилгексилокси)-1,4-фенилен винилен] (MEH-PPV) с координационным олигомером (Pt$_{0.75}$C$_{60}$)$_n$ и сопоставлен с ФПЗ в смесях MEH-PPV/C$_{60}$. С меси были изучены методами спектроскопии оптического поглощения, рассеяния света, фотолюминесценции, фотоиндуцированного поглощения и возбуждения фототока. Обнаружено, что эффективность ФПЗ в смеси MEH-PPV/(Pt$_{0.75}$C$_{60}$)$_n$ несколько ниже, чем в MEH-PPV/C$_{60}$. Эта различие отнесено к более выраженному разделению фаз в MEH-PPV/(Pt$_{0.75}$C$_{60}$)$_n$ на наномасштабе. Тем не менее, данные фототоковых измерений предполагают, что цепи (Pt$_{0.75}$C$_{60}$)$_n$ могут обеспечить сбор фотоиндуцированных зарядов.

Conjugated polymers are promising materials for photonics and electronics including photovoltaic applications. One of the most studied polymer based material for photovoltaics today is a donor-acceptor blend of a soluble conjugated polymer, e.g. poly[2-methoxy-5-(2′-ethyl-hexyloxy)-1,4-p henylene vinylene] (MEH-PPV), with a soluble derivative of fullerene [1]. In such a blend, photons generate excitons at the conjugated polymer, which dissociate into free electrons and holes at the polymer/fullerene interface in the PCT reaction. Fullerenes and their derivatives are well known to be the most effective acceptors in PCT [2]. Essentially that fullerenes in these blends can form a highly conductive network for collection of photoinduced charges that makes fullerenes indispensable in bulk-heterojunction polymer solar cells. However, the optimized active layer of such a cell comprises up to 80 % of fullerene [1], which almost does not absorb light in the solar cell. In this work, we study PCT in blends of MEH-PPV with a fullerene-based coordination oligomer (Pt$_{0.75}$C$_{60}$)$_n$. Our motivation was that
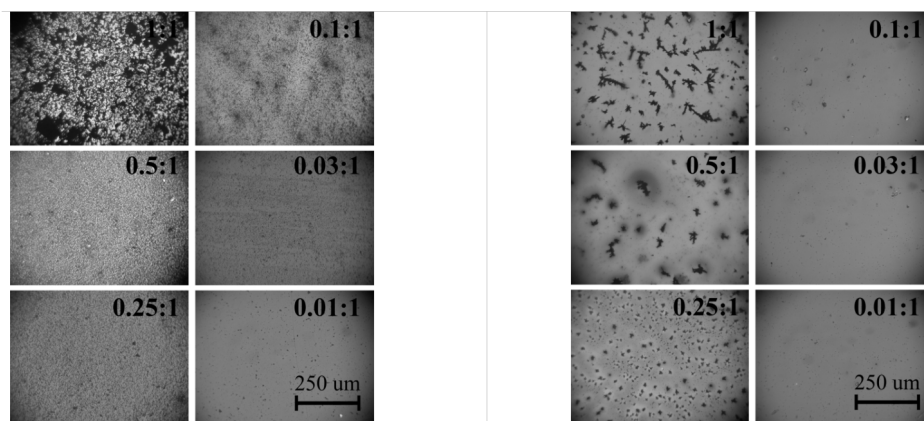
Fig. 1. Microphotographs of MEH-PPV/$Pt_{0.75}C_{60}$ (left) and MEH-PPV/C_{60} (right) blends with different acceptor:donor ratio shown in each photo.

$(Pt_{0.75}C_{60})_n$ chains could facilitate charge transport in bulk heterojunction devices allowing decreasing the fullerene content in it. Meanwhile, $(Pt_{0.75}C_{60})_n$ is expected to charge donor-acceptor phase separation peculiarities essentially influencing charge collection in bulk heterojunction devices [1]. We characterized MEH-PPV/$(Pt_{0.75}C_{60})_n$ blended films by using optical absorption and scattering technique, and then investigated their photophysical properties by using photoluminescence (PL), photoinduced absorption (PIA), and photocurrent spectroscopy methods. We also studied MEH-PPV/C_{60} blends and compare their properties with those of MEH-PPV/$(Pt_{0.75}C_{60})_n$.

Sample preparation: $(Pt_{0.75}C_{60})_n$ was synthesized by reaction of C_{60} with $Pt(dba)_2$ (dba = dibenzylideneacetone) with molar ratio $Pt(dba)_2/C_{60} = 3/4$ according to [3]. The compound was characterized by elemental analysis, IR, and Raman spectroscopies.

Drop-cast films of MEH-PPV/$(Pt_{0.75}C_{60})_n$ and MEH-PPV/C_{60} blends were prepared from chlorobenzene for molar acceptor:donor ratios in the range 0.0001−1. The solutions were treated in ultrasonic bath before drop-casting.

For photoelectric studies we fabricated photodiodes in the sandwich structure. Films of MEH-PPV/acceptor blends were drop-cast on ITO-coated glass substrates. Then a top Al-electrode was thermally deposited. The active area of the devices was ≈ 0.1 cm^2. Thicknesses of the films were estimated as ~200 nm from their optical density.

Light absorption and scattering. Optical absorption spectra of MEH-PPV/acceptor blends were measured by using a spectrophotometer. In order to evaluate separately the absorption and scattering contribution in the measured optical density of the films, we elaborated a simple technique described elsewhere [4]. Briefly, we measured the laser beam transmission just behind the polymer film at 532 and 633 nm by using a wide-aperture photodetector with and without a small damp placed in front of the photodetector to block the straight laser light.

PIA and PL. In PIA spectroscopy, the measured signal is fractional change in the sample transmission (dT/T) induced by a pump beam. The pump beam was mechanically chopped and the PIA signal in the probe channel was processed by a lock-in amplifier at modulation frequency f. In the probe channel, we used a tungsten-halogen lamp illuminating the sample, a monochromator, and solid-state photodetectors (Si and InGaAs). As a pump source, we used second harmonic radiation of a cw Nd:YAG laser (532 nm). PIA data were obtained at ambient conditions or under nitrogen flow in the temperature range 100−300 K. For PL measurements, we used the same set up without the probe beam. The PL spectra were recorded in the backscattering geometry at ambient conditions in the range 550−770 nm. The PL intensity was normalized to that of pristine MEH-PPV. The PL data were also normalized to the sample absorption at 532 nm evaluated from the sample optical transmission.

Photocurrent measurements. In photocurrent measurements, optical radiation from a tungsten halogen lamp dispersed by a monochromator was chopped at ~114 Hz with power on the sample no more than 0.25μW. The photocurrent was measured by a lock-in amplifier. We took into account the spectral response of the excitation lamp and the

spectral transmission function of the experimental set-up. The photocurrent studies were done in ambient conditions.

Microscopy, absorption and scattering data. Fig. 1 shows microphotographs of MEH-PPV/$Pt_{0.75}C_{60}$ and MEH-PPV/C_{60} films. It is seen that for acceptor concentration higher than 10 % both $(Pt_{0.75}C_{60})_n$ and C_{60} form their own phase in the blends resulting in a more inhomogeneous film. For acceptor concentration higher than 20 %, film's orangish red color resulting from MEH-PPV absorption weakened and fully disappeared in the 1:1 blends. At low acceptor concentration (<10 %), optical absorption spectra of MEH-PPV/$Pt_{0.75}C_{60}$ blends were similar to those of MEH-PPV/C_{60}. Typical absorption spectra of a 1:0.2 MEH-PPV/$Pt_{0.75}C_{60}$ blend is shown in Fig. 5. For higher $(Pt_{0.75}C_{60})_n$ concentration, light scattering gave a noticeable contribution to the optical transmission of the films impeding the optical absorption measurement.

We evaluated both optical absorption (αd) and Rayleigh scattering (σd) to the measured optical density (OD) of a blended film with thickness d by using the technique described above. Fig. 2 shows the results at 532 nm. It is seen that the contribution of σd to the OD gradually increases with $(Pt_{0.75}C_{60})_n$ concentration whereas the αd decreases. Similar dependencies were measured at 633 nm, but both the αd and σd curves were close to each other monotonically increasing from zero with $(Pt_{0.75}C_{60})_n$ concentration. It seems that the noticeable absorption of MEH-PPV/$Pt_{0.75}C_{60}$ at 633 nm is due to $(Pt_{0.75}C_{60})_n$. On the other hand, for MEH-PPV/C_{60} blends, both the αd and σd at 633 nm were below the experimental error (~0.1).

Thus, our light scattering and microscopy data suggest that the characteristic size of optical inhomogeneity in MEH-PPV/$Pt_{0.75}C_{60}$ blends is considerably closer to the optical wavelength than that in MEH-PPV/C_{60} blends. Fullerene molecules form large separated features observed optically at high fullerene concentration (Fig. 1, right). Therefore, we suppose that essentially different morphologies of MEH-PPV/$Pt_{0.75}C_{60}$ and MEH-PPV/C_{60} blends at the microscale can lead to their different photophysical properties.

PL data. The efficiency of PL quenching in donor-acceptor blends is determined by the ratio between the characteristic lengths
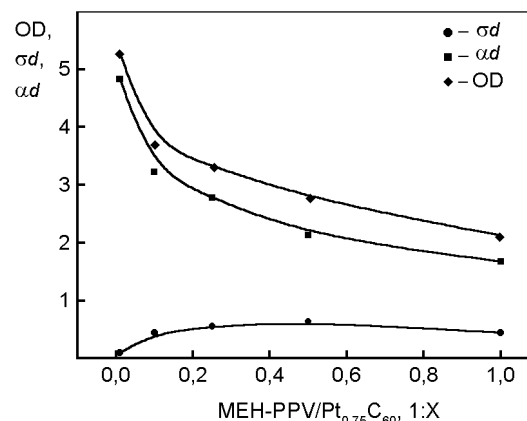

Fig. 2. Scattering (σd) and absorption (αd) contributions to the measured optical density (OD = σd + αd) for MEH-PPV/$Pt_{0.75}C_{60}$ films vs acceptor: donor ratio at 532 nm. The lines are guides to the eye.

of singlet exciton diffusion and of phase separation. The shorter the latter, the more efficient PL quenching will be. We have observed that $(Pt_{0.75}C_{60})_n$ strongly quenches MEH-PPV PL. Fig. 3 compares PL quenching efficiency in MEH-PPV/$Pt_{0.75}C_{60}$ and MEH-PPV/C_{60} blends. One can see that both acceptors display strong PL quenching at low acceptor content <0.01 %; however, the quenching efficiency in MEH-PPV/$Pt_{0.75}C_{60}$ is 5–8 times less than in MEH-PPV/C_{60} at acceptor concentrations ≤20 %. We suggest that the most possible reason of this difference is due to more pronounced phase separation in MEH-PPV/$Pt_{0.75}C_{60}$ blends as compared with MEH-PPV/C_{60}. In fact, $(Pt_{0.75}C_{60})_n$ is insoluble and can form relatively large aggregates at the nanoscale whereas fullerene molecules are expected to give more intimate mixing with MEH-PPV chains. As a result, a singlet exciton photoexcited at MEH-PPV has to travel a longer path to the donor/acceptor interface in the MEH-PPV/$Pt_{0.75}C_{60}$ than in MEH-PPV/C_{60}.

The shape of the PL quenching curves in Fig. 3 is essentially different for C_{60} and $(Pt_{0.75}C_{60})_n$ that can also be attributed mainly to the difference in characteristic phase separation lengths in both types of blends.

Note that MEH-PPV/C_{60} blends demonstrate some increase in the normalized PL at acceptor concentration >20 % (Fig. 3). The reasons of this are unclear. We believe that this is not an artefact of PL normalization to the absorbed power pump since the
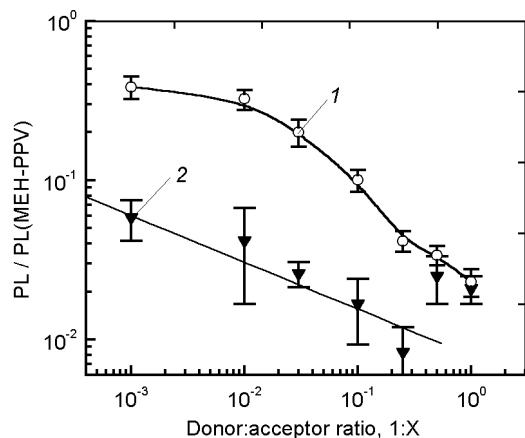
494

Fig. 3. PL quenching in MEH-PPV/Pt$_{0.75}$C$_{60}$ (*1*) and MEH-PPV/C$_{60}$ (*2*) blends vs acceptor:donor ratio referenced to pristine MEH-PPV PL. Solid lines are a guide to the eye. All values are normalized to the absorbed pump power at 532 nm.

unnormilzed PL also increased with C$_{60}$ content. Moreover, we rather overestimate the pump power absorbed by MEH-PPV in both types of blends mainly because of dropping MEH-PPV absorption at high acceptor content.

PIA data. PIA spectroscopy in conjugated polymers probes mainly two types of long-lived photoexcitations: triplet excitons and polarons. If the former are neutral, the latter are charged and, therefore, can be used to monitor PCT. Fig. 4 summarizes our PIA data for 1:0.03 MEH-PPV/Pt$_{0.75}$C$_{60}$ and MEH-PPV/C$_{60}$ blends measured under the same experimental conditions. Fig. 4a shows PIA spectra of both blends. One can see that PIA absorption spectra have nearly

the same shape. Both spectra show high (1.3 eV) and low (<0.8 eV) energy bands assigned to polarons at MEH-PPV [5]. The high-energy band has two features at 1.2 and 1.3 eV attributed to 0–0 and 0–1 vibrational sidebands [6]. As the low-energy band in MEH-PPV peaks at 0.4 eV [6], we could observe only its high-frequency tail within our spectral range (Fig. 4a). Because of this, we will analyze only the high-energy band. As Fig. 4a shows, long-lived charge separated states are effectively excited in both blends; meanwhile, the PIA signal at 1.3 eV in MEH-PPV/C$_{60}$ is ~2 times higher as compared to MEH-PPV/Pt$_{0.75}$C$_{60}$. This ratio was nearly the same for all the pump intensities studied.

The frequency dependence of the PIA signal can provide information about the lifetime of photoexcitations. If they follow a monomolecular kinetics with lifetime τ, the frequency dependence of the PIA is

$$\frac{dT}{T} \propto \frac{1}{1 + i2\pi f \tau}. \qquad (1)$$

In pristine MEH-PPV, triplet excitons are known to dominate in PIA at low temperature (~100 K) giving a band at 1.35 eV with the monomolecular kinetics [6, 7]. On the other hand, polarons in PPV-type conjugated polymers show a power-law frequency dependence $1/f^{\alpha}$ with $\alpha \sim 0.5$ [6]. This dependence is usually interpreted as a result of "dispersive" recombination implying a broad distribution in polaron lifetimes and can be fit by the empirical Cole-Cole model [8, 9]
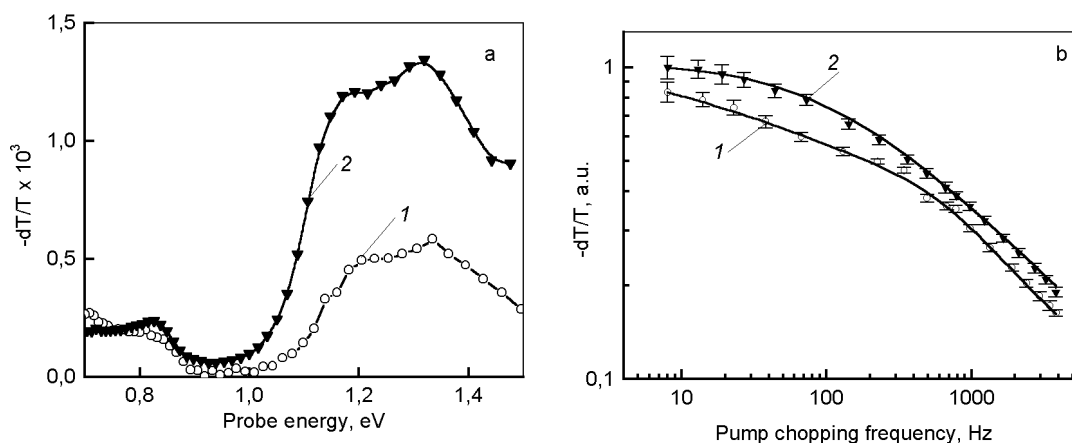

Fig. 4. PIA data for 1:0.03 MEH-PPV/Pt$_{0.75}$C$_{60}$ (*1*) and MEH-PPV/C$_{60}$ (*2*) blends recorded for pump intensity 1 W/cm^2 at 110 K. Almost all the pump power was absorbed in the films. (a) PIA spectra for chopping frequency 70 Hz. The lines are a guide to the eye. (b) Normalized frequency dependences. Solid lines are fits to the data (see the text).

$$\frac{dT}{T} \propto \frac{1}{1 + (i2\pi f\tau)^\alpha}.\qquad (2)$$

Fig. 4b compares frequency dependences of the peak at 1.3 eV for 1:0.03 MEH-PPV/$Pt_{0.75}C_{60}$ and MEH-PPV/C_{60} blends. It is seen that they are quite different. "Dispersive" kinetics according to Eq.(2) with $\alpha = 0.44$ and $\tau = 12$ ms gave a good fit to the experimental data for MEH-PPV/C_{60} (Fig. 4b, solid line). For MEH-PPV/$Pt_{0.75}C_{60}$ blends, the frequency dependence had a characteristic knee (Fig. 4b), and any single "dispersive" kinetics (Eq.(2)) did not give a satisfactory fit for all the donor/acceptor ratios studied. We relate this to the contribution of MEH-PPV triplet excitons in the PIA band at 1.3 eV. A superposition of "dispersive" and monomolecular kinetics gave a good approximation to the frequency dependence for all the MEH-PPV/$Pt_{0.75}C_{60}$ blends. The lower line in Fig. 4b shows such a bimodal fit by the sum of "dispersive" ($\alpha = 0.35$, $\tau = 11$ ms) and monomolecular ($\alpha = 1$, $\tau = 1.5$ ms) kinetics (Eq.(2)). Therefore, our PIA data suggest that MEH-PPV triplet excitons in MEH-PPV/$Pt_{0.75}C_{60}$ blends are not completely quenched in contrast to MEH-PPV/C_{60} blends. This is also supported by the PL quenching data in Fig. 2 showing that the PL in the 1:0.03 MEH-PPV/$Pt_{0.75}C_{60}$ blend is quenched only by a factor of 5. Therefore, a part of singlet excitons lives a sufficient time to be converted into triplet ones via intersystem crossing.

Photocurrent action spectra. Fig. 5 demonstrates photocurrent action and optical absorption spectra for 1:0.2 MEH-PPV/$Pt_{0.75}C_{60}$ blend. It is seen that the former closely follows the absorption edge of MEH-PPV implying that photoexcitations at MEH-PPV dissociate into free carriers in the bulk heterojunction as it occurs in MEH-PPV/C_{60} blends. The peak responsivity of the photodiode was 3.4 mA/W at 505 nm that corresponds to the external quantum efficiency about 1 %. This efficiency is essentially lower than that of typical MEH-PPV/C_{60} devices. At this point, we can not compare the efficiency of charge collection in MEH-PPV/C_{60} and MEH-PPV/$(Pt_{0.75}C_{60})_n$ devices since the latter were not optimized on donor/acceptor ratio, preparation condition, etc.

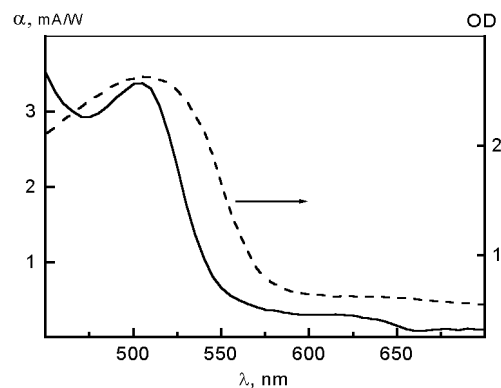In conclusion, we have done comparative studies of optical and photophysical proper-

Fig. 5. Photocurrent action spectra (solid) and optical density (dashed) for the photodiode with 1:0.2 MEH-PPV/$Pt_{0.75}C_{60}$ working layer.

ties of MEH-PPV/$Pt_{0.75}C_{60}$ and MEH-PPV/C_{60} blends. Their optical characterization has shown that the morphology of the blends is essentially different at the microscale. By using PL and PIA spectroscopy, we have found that the efficiency of PCT in MEH-PPV/$Pt_{0.75}C_{60}$ is about 2 times lower than in MEH-PPV/C_{60}. We attribute this difference to higher phase separation in MEH-PPV/$Pt_{0.75}C_{60}$ at the nanoscale. Meanwhile, our photocurrent spectra indicate that $(Pt_{0.75}C_{60})_n$ could collect the photoinduced charges.

References

1. C.J.Brabec, N.S.Sariciftci, J.C.Hummelen, *Advanced Functional Materials*, **11**, 15 (2001).
2. N.S.Sariciftci, L.Smilowitz, A.J.Heeger et al., *Science*, **258**, 1474 (1992).
3. H.Nagashima, Y.Kato, H.Yamaguchi et al., *Chem. Lett.*, 1207 (1994).
4. S.G.Elizarov, A.E.Ozimova, D.Yu.Paraschuk et al., *Proc. SPIE*, **6257**, 293 (2006).
5. H.S.Woo, S.C.Graham, D.A.Halliday et al., *Phys. Rev. B*, **46**, 7379 (1992).
6. X.Wei, Z.V.Vardeny, N.S.Sariciftci et al., *Phys. Rev. B*, **53**, 2187 (1996).
7. D.S.Ginger, N.C.Greenham, *Phys. Rev. B*, **59**, 10622 (1999).
8. O.Epshtein, G.Nakhmanovich, Y.Eichen et al., *Phys. Rev. B*, **63**, 125206 (2001).
9. A.Bello, E.Laredo, M.Grimau, *Phys. Rev. B*, **60**, 12764 (1999).

Фотоіндукований перенос заряду у донорно-акцепторній суміші MEH-PPV/Pt$_{0.75}$C$_{60}$

А.А.Бакулин, С.Г.Єлізаров, А.Е.Озімова, Д.Ю.Паращук, Ю.М.Новіков, М.В.Цікалова, С.А.Арнаутов, Е.М.Нечволодова

Досліджено фотоіндукований переніс заряду (ФПЗ) в донорно-акцепторних сумішах полі[2-метокси-5-(2'-этилгексилокси)-1,4-фенілен вінілен] (MEH-PPV) з координаційним олігомером (Pt$_{0,75}$C$_{60}$)$_n$ і зіставлено з ФПЗ у сумішах MEH-PPV/C$_{60}$. Ці суміші вивчено методами спектроскопії оптичного поглинання, розсіяння світла, фотолюмінесценції, фотоіндукованого поглинання і збудження фотоструму. Виявлено, що ефективність ФПЗ у суміші MEH-PPV/(Pt$_{0,75}$C$_{60}$)$_n$ декілька нижче, ніж у MEH-PPV/C$_{60}$. Ця відмінність пов'язана з більш вираженим розподілом фаз у MEH-PPV/(Pt$_{0,75}$C$_{60}$)$_n$ на наномасштабі. Проте, дані вимірювань фотострумів припускають, що ланцюги (Pt$_{0,75}$C$_{60}$)$_n$ можуть забезпечити збір фотоіндукованих зарядів.